Jordan Journal of Civil Engineering, Volume **16**, No. **3**, **2022**

Dynamic Analysis of High-speed Railway Bridges Applying Bridge-Vehicle Interaction

Abdallah Salama [1)]***, Atef Eraky*** [2)]***, Muhammed Yahya*** [3)*] ***and Rania Samir*** [4)]

[1)] PhD, Department of Structural Engineering, Faculty of Engineering, Zagazig University, Zagazig, Egypt. E-Mail: eng_abdullah203@yahoo.com
[2)] Professor, Department of Structural Engineering, Faculty of Engineering, Zagazig University, Zagazig, Egypt. E-Mail: atef_eraky@yahoo.com
[3)*] Teaching Assistant, Department of Structural Engineering, Faculty of Engineering, Zagazig University, Zagazig, Egypt. * Corresponding Author. E-Mail: myehia@zu.edu.eg
[4)] Associate Professor, Department of Structural Engineering, Faculty of Engineering, Zagazig University, Zagazig, Egypt. E-Mail: raniasamir02@gmail.com

ABSTRACT

The problem of train passage over bridges is an interaction problem between two systems; the bridge system including track and the passing train system. To consider the bridge-vehicle interaction, a non-linear problem shall be solved, because the response of each system depends on the response of the other system simultaneously. Two ways of solving the interaction problem are applied in an FE numerical domain, where the first way treats the two systems as one whole system, which dynamically updates its stiffness matrix, while the second way considers the transferred forces at contact points between two decoupled systems with constraint equations. The bridge system is modeled as 2D Bernoulli beams and the track as a single continuous non-viscous elastic layer beneath rails with irregularities, whereas the train system is modeled as separate moving systems with each system having two degrees of freedom (DOFs) and consisting of a lumped mass supported by one layer of suspension system that comprises a spring-damper unit. The parametric study on a non-prismatic continuous prestressed concrete bridge using a high-speed train shows that the interaction models give similar responses to moving-load model except at resonance speeds for which conservative values and higher resonance speeds are given.

KEYWORDS: High-speed train, Railway bridge, Train-bridge interaction, Dynamic analysis, Resonance.

INTRODUCTION

High-speed railway networks have become of great interest due to the advances in the locomotives' industry enhanced by the economic and social demands and railway bridges are an important part of these networks. The problem of vibration of beams under moving loads reached a theoretical formulation in the beginnings of the 20th century and Timoshenko (1955) introduced a solution for the problem. An in-depth study was carried out by Frýba (1999) including the case of a spring-damper system and a two-axle coach traversing the beam. The introduction of high-speed trains that began in the second half of the 20th century required a more careful dynamic study rather than depending on the static impact factor to account for the increase of response caused by the dynamic interaction. When the train mass is small compared to that of the bridge, ignoring the inertial properties of the train can lead to a simple case in which bridge response can only be obtained, but in other cases, an adequate modeling for the train as a subsystem is required in the dynamic analysis (Yang et al., 2004). A four-DOFs system for modeling train coach including the pitching effect was studied by Yang et al. (1999), while a reduced model of two DOFs for the train system was utilized by

Received on 17/6/2021.
Accepted for Publication on 2/4/2022.

Atashafrazeh and Shirmohammadi (2016) to investigate the effect of wheel flatness on high-speed railway track behavior. Xia et al. (2003) studied the interaction between the bridge and the high-speed articulated train system that comprises transverse and vertical connections between car bodies and two suspension layers with the whole train system containing 115 DOFs. Olmos and Astiz (2018) also adopted a 3D articulated train system in the interaction problem to assess running safety under wind action. Full 2D representation of a conventional train with 10 DOFs for the car body and the two suspension systems has been applied with track structure included to evaluate the response and riding comfort (Wu and Yang, 2003). Zhang et al. (2001) applied a 3D model for the train and bridge with car body and suspensions having 20 DOFs, while Wu et al. (2001) used a 3D model for car body and suspensions with a total of 27 DOFs for each car body. Many techniques of solution have been developed by researches for the coupled nonlinear interaction problem. Iterative solutions have been widely used (Delgado and Santos, 1997; Lei and Noda, 2002; Yang and Fonder, 1996). Delgado and Santos (1997) used an iterative solution which treats the train as a moving system on an immovable bridge system which serves as a base for the train structure and the bridge deflections are considered settlement of supports for the moving system with convergence criteria for the transferred dynamic forces between the two systems. Another way of solution was proposed by Lou (2005) making use of the potential energy with the stationary value principle for the whole system. Zeng et al. (2016) utilized the energy principle and used the pseudo-excitation method to formulate the excitation vectors between wheels and rails. Yang et al. (1995) introduced a technique based on the dynamic condensation of the DOFs related to the lower part of the car body system to those of the bridge with which they are in contact. Many other researchers utilized the way of two decoupled systems with contact forces and constraint equations of no-wheel-separation at contact points (Nour & Issa, 2016; Yang et al., 2004). The allowance for wheel separation was further studied by Neves et al. (2014). Gu (2015) introduced a solution method called structural articulation, in which the bridge and the train form a single virtual system. An excellent discussion about the evolution of interaction problem modeling and track modeling was held by Zhai et al. (2019). In this work, two ways for interaction simulation will be adopted. The first is a non-iterative procedure which avoids the decoupling of the two systems or applying convergence criteria, but deals with the train and the bridge as one whole system with its stiffness matrix being updated at each time step. The second procedure utilizes the decoupling of two systems with contact forces and convergence criteria for the dynamic part of contact forces.

MODELING OF BRIDGE AND TRAIN SYSTEMS

Bridge is discretized into elements represented by 2D Bernoulli beams with 4 DOFs for each element. Elements of variable height and variable uniform mass are used to model non-prismatic prestressed concrete bridges. The matrices of the bridge system are assembled from element matrices of stiffness and consistent mass with Rayleigh damping applied for the damping matrix. The Full 2D model representing the car body and its suspensions includes 10 DOFs, as shown in Fig. 1.a, where u_w denotes wheel transitional DOF, u_b and r_b denote bogie transitional and rotational DOFs, respectively, while u_c and r_c denote car body transitional and rotational DOFs, respectively. However, the reduced model containing the half lumped mass of the car body and one equivalent suspension layer, as shown in Fig. 1.b, is used in this study for its simplicity and its ability to give the extreme response of the train, whereas the other model gives the response of the central point of the car body which is usually less than the response of both ends. The two DOFs of the reduced model are the displacements of the lumped mass u_v and the wheel u_w. Dynamic analysis will be performed making use of the high-speed load model (HSLM), recommended by the European Rail Research Institute (ERRI) committee (ERRI, 1999), which is intended to realize the signature of real present and prospective high-speed trains. The HSLM represents the configuration of an articulated train that comprises starting and ending power cars, two end coaches and a number of intermediate coaches. EN 1991-2 (2003) proposed the HSLM-A family that includes 10 models with axle weight (P) varying from 170 to 210 kN and variable length and number for

coaches, as shown in Fig. 2. Track structure is modeled as a single continuous non-viscous elastic layer beneath rails, as shown in Fig. 3 and irregularities are defined as power spectral densities (PSDs) with different classes (Podwórna, 2015).

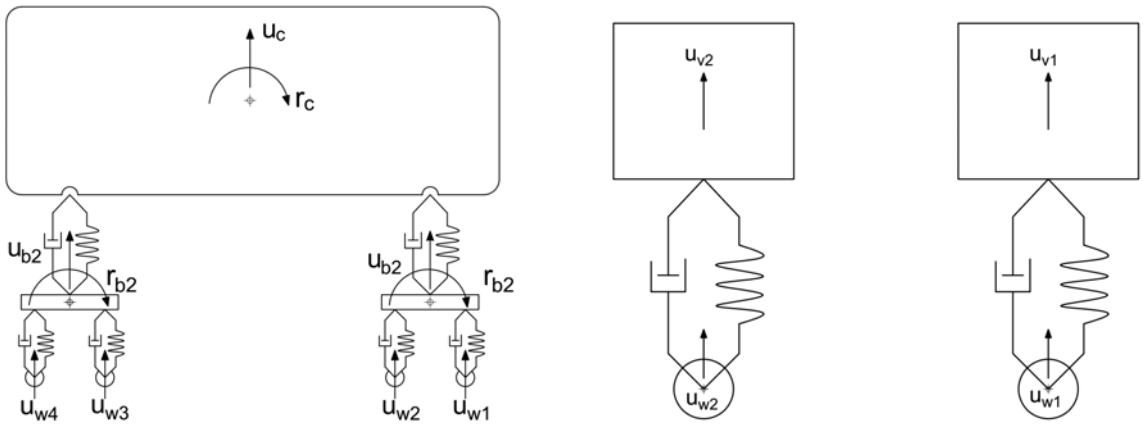

(a) (b)

Figure (1): (a) Full model of car body and suspensions and (b) Reduced model of lumped mass and one suspension layer

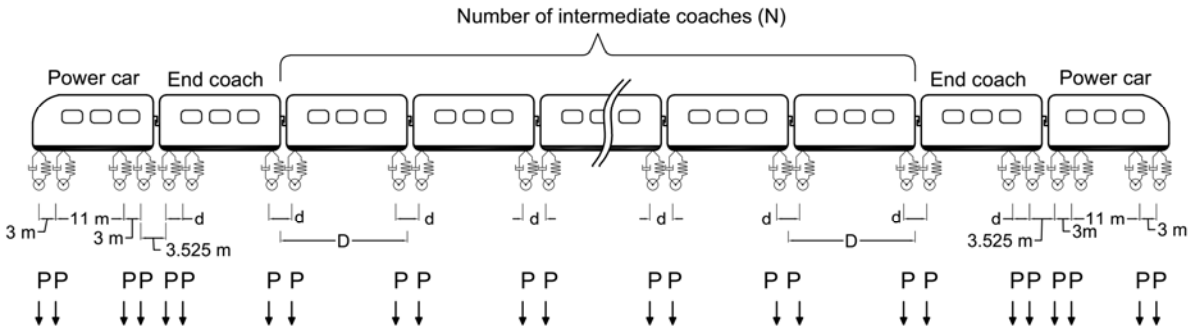

Figure (2): HSLM configuration

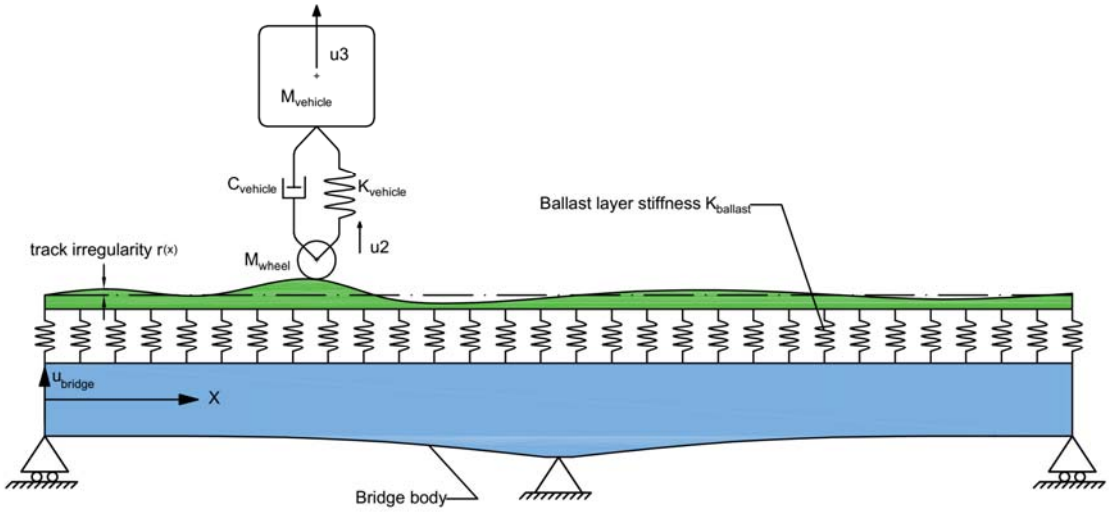

Figure (3): Bridge and track structure

BRIDGE-VEHICLE INTERACTION PROBLEM

The general coupled equation that describes the interaction problem is as given in Eq. (1).

$$\begin{bmatrix} M_{bridge} & 0 \\ 0 & M_{vehicle} \end{bmatrix} \begin{Bmatrix} \ddot{U}_{bridge} \\ \ddot{U}_{vehicle} \end{Bmatrix} + \begin{bmatrix} C_{bridge} & 0 \\ 0 & C_{vehicle} \end{bmatrix} \begin{Bmatrix} \dot{U}_{bridge} \\ \dot{U}_{vehicle} \end{Bmatrix} + \begin{bmatrix} K_{bridge} & 0 \\ 0 & K_{vehicle} \end{bmatrix} \begin{Bmatrix} U_{bridge} \\ U_{vehicle} \end{Bmatrix} = \begin{Bmatrix} F_{bridge} \\ F_{vehicle} \end{Bmatrix} \quad (1)$$

Coupling comes from the dependency of $F_{vehicle}$ and F_{bridge} on the deformation of both bridge and vehicle simultaneously at one time step. $F_{vehicle}$ and F_{bridge} are equal forces, but in opposite directions; hence, the term $f_{contact}$ will be used to represent the transferred contact force between the two systems. The contact force is divided into a static part (f_{stat}) representing the weight of the axle and a dynamic part (f_{dyn}) representing the interaction induced force, as indicated in Eq. (2).

$$f_{contact} = f_{dyn} + f_{stat} \quad (2)$$

The vehicle system, which is connected to the bridge body through the track elastic property as in Fig. 4, has the following equations of motion:

$$f_{dyn} - K_{ballast}(u_1 - u_2) = 0 \quad (3)$$

$$-K_v(u_2 - u_3) - C_v(\dot{u}_2 - \dot{u}_3) - K_{ballast}(u_2 - u_1) = M_w \times \ddot{u}_2 \quad (4)$$

$$-K_v(u_3 - u_2) - C_v(\dot{u}_3 - \dot{u}_2) = M_v \times \ddot{u}_3 \quad (5)$$

where: $K_{ballast}$ is the stiffness of ballast layer under vehicle/train wheels, K_v is the stiffness of suspension, C_v is the damping of suspension, M_v is the mass representing the train coach and u_1, u_2 and u_3 are the deformations of the contact point, wheel and suspended mass, respectively. It is worth noting that u_2 and u_3 are measured from the position of initial setting in the vehicle system and the track due to the own weight of the vehicle ($P = [M_v+M_w]\ g$).

Combining the last three equations (3-5) leads to the vehicle system equation given as shown in Eq. (6):

$$\begin{bmatrix} 0 & 0 & 0 \\ 0 & M_w & 0 \\ 0 & 0 & M_v \end{bmatrix} \begin{Bmatrix} \ddot{u}_1 \\ \ddot{u}_2 \\ \ddot{u}_3 \end{Bmatrix} + \begin{bmatrix} 0 & 0 & 0 \\ 0 & C_v & -C_v \\ 0 & -C_v & C_v \end{bmatrix} \begin{Bmatrix} \dot{u}_1 \\ \dot{u}_2 \\ \dot{u}_3 \end{Bmatrix} + \begin{bmatrix} K_{ballast} & -K_{ballast} & 0 \\ -K_{ballast} & K_v + K_{ballast} & -K_v \\ 0 & -K_v & K_v \end{bmatrix} \begin{Bmatrix} u_1 \\ u_2 \\ u_3 \end{Bmatrix} = \begin{Bmatrix} f_{dyn} \\ 0 \\ 0 \end{Bmatrix} \quad (6)$$

Two models for the train/vehicle are adopted in this study. The first model applies the simple representation for the train axles as a series of moving loads ignoring the inertial effects of the train; hence, this simple model is associated with a non-interaction problem which is solved through direct time integration under the action of moving loads. The other model applies the lumped masses with one suspension layer, as shown in Fig. 1.b, which is solved through the two forthcoming methods.

PROPOSED METHODS OF SOLUTION

In the proposed interaction methods in this work, some assumptions are followed: *i*) track stiffness is constant under the two rails, *ii*) track damping is negligible, *iii*) no separation occurs between the wheel and the track; the wheel is in permanent contact with the rails, *iv*) friction forces at contact points are neglected.

In the two forthcoming methods, direct integration using Newmark's β method (applying values $\gamma = 1/2$ and $\beta = 1/4$; a constant average acceleration method) will be applied for time integration (Newmark, 1959).

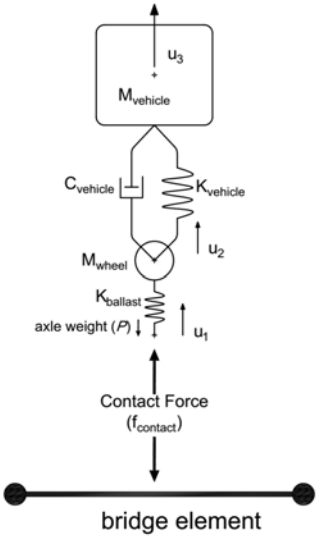

Figure (4): Vehicle system connected to the bridge by track elastic property

The first method of solution for the interaction problem deals with the entire system that includes both

the bridge and the vehicle. The entire system matrices are updated according to the position of various moving axles at each time step. The contact forces between the axles and the bridge are internal forces; consequently, they don't appear in the force matrix and only the weights of passing axles are included in the force matrix. In this method, it is a necessity that the axles of the train move from node to node at each step and it is not allowed for a wheel to be in-between two nodes; the lower node of the axle must coincide with a node of the bridge. This requires that the time step is governed by both train speed and bridge element size. Fine mesh of bridge structure is then used to assure a good level of accuracy. When a vehicle axle coincides with node *i* of the bridge, that has *n* nodes, the stiffness matrix elements associated with this node are updated. System mass and damping matrices remain constant at each time step unless the damping in the track structure is required to be included in the analysis. Force matrix is formulated by adding the axle weight *P* to the corresponding DOF of node *i*. The updated stiffness matrix takes the form:

$$\begin{bmatrix} k_{11} & k_{12} & \cdots & \cdots & k_{(1)(2i-1)} & k_{(1)(2i)} & \cdots & k_{(1)(2n)} & 0 & 0 \\ k_{21} & k_{22} & k_{23} & \cdots & k_{(2)(2i-1)} & k_{(2)(2i)} & \cdots & k_{(2)(2n)} & 0 & 0 \\ \vdots & k_{32} & k_{33} & \cdots & k_{(3)(2i-1)} & k_{(3)(2i)} & \cdots & k_{(3)(2n)} & 0 & 0 \\ \vdots & \vdots & \vdots & \ddots & \vdots & \vdots & & & 0 & 0 \\ k_{(2i-1)(1)} & k_{(2i-1)(2)} & k_{(2i-1)(3)} & \cdots & k_{(2i-1)(2i-1)} + k_{ballast} & \vdots & & & -k_{ballast} & 0 \\ k_{(2i)(1)} & k_{(2i)(2)} & k_{(2i)(3)} & \cdots & \cdots & k_{(2i)(2i)} & & & 0 & 0 \\ \vdots & \vdots & \vdots & & & & \ddots & & 0 & 0 \\ k_{(2n)(1)} & k_{(2n)(2)} & k_{(2n)(3)} & & & & & k_{(2n)(2n)} & 0 & 0 \\ 0 & 0 & 0 & 0 & -k_{ballast} & 0 & 0 & 0 & k_v + k_{ballast} & -k_v \\ 0 & 0 & 0 & 0 & 0 & 0 & 0 & 0 & -k_v & k_v \end{bmatrix}$$

If the damping in the track is intended to be included in the analysis, the damping matrix of the whole system shall also be updated in a similar manner as the stiffness matrix at each time step. This method of solving the non-linear interaction problem is a fast and non-iterative method; hence, it has the advantage of simplicity, but it requires a small size of elements in bridge discretization for accuracy.

The second method of solution applies decoupling of the two systems with transferred contact force between them and a constraint equation of permanent contact (no jumps). Convergence criteria for the dynamic part of contact forces are used to maintain the required accuracy. This method is based on partitioning the vehicle axle with attached spring system in Eq. (6) into:

$$\begin{bmatrix} M_{ll} & M_{lu} \\ M_{ul} & M_{uu} \end{bmatrix} \begin{Bmatrix} \ddot{U}_l \\ \ddot{U}_u \end{Bmatrix} + \begin{bmatrix} C_{ll} & C_{lu} \\ C_{ul} & C_{uu} \end{bmatrix} \begin{Bmatrix} \dot{U}_l \\ \dot{U}_u \end{Bmatrix} + \begin{bmatrix} K_{ll} & K_{lu} \\ K_{ul} & K_{uu} \end{bmatrix} \begin{Bmatrix} U_l \\ U_u \end{Bmatrix} = \begin{Bmatrix} F_l \\ F_u \end{Bmatrix} \tag{7}$$

where: $M_{ll} = [0]$, $M_{uu} = \begin{bmatrix} M_w & 0 \\ 0 & M_v \end{bmatrix}$, $M_{lu} = \langle 0 \quad 0 \rangle$, $M_{ul} = M_{lu}^T$,

$C_{ll} = [0]$, $C_{uu} = \begin{bmatrix} C_v & -C_v \\ -C_v & C_v \end{bmatrix}$, $C_{lu} = \langle 0 \quad 0 \rangle$, $C_{ul} = C_{lu}^T$,

$K_{ll} = [k_{ballast}]$, $K_{uu} = \begin{bmatrix} k_v + k_{ballast} & -k_v \\ -k_v & k_v \end{bmatrix}$, $K_{lu} = \langle -k_{ballast} \quad 0 \rangle$, $K_{ul} = K_{lu}^T$,

$U_l = \{u_1\}$, $\dot{U}_l = \{\dot{u}_1\}$, $\ddot{U}_l = \{\ddot{u}_1\}$, $F_l = \{f_{dyn}\}$, $U_u = \begin{Bmatrix} u_2 \\ u_3 \end{Bmatrix}$, $\dot{U}_u = \begin{Bmatrix} \dot{u}_2 \\ \dot{u}_3 \end{Bmatrix}$, $\ddot{U}_u = \begin{Bmatrix} \ddot{u}_2 \\ \ddot{u}_3 \end{Bmatrix}$, $F_u = \begin{Bmatrix} 0 \\ 0 \end{Bmatrix}$,

and an iterative algorithm is used to get the response of the vehicle system and then, the contact force transferred to the bridge system is calculated, which in turn is solved to get its response.

The solution algorithm is as follows:

1. Bridge data (material properties and geometry of the

bridge) is read; then, the bridge is discretized into finite elements. Each element has an inertia and distributed mass used to create the element matrices.

2. For the bridge system, the system matrices (K, M) are assembled.
3. Modal analysis is applied to the bridge system to get its fundamental natural frequencies.
4. Damping matrix (Rayleigh damping) of the bridge is constructed from the first two natural frequencies (ω_1, ω_2), as in Eq. (8), where ζ is the damping ratio. Damping ratio will be taken 1% for prestressed concrete bridges.

$$[C] = a_0[M] + a_1[K] \quad (8)$$

where: $a_0 = \frac{2\zeta\omega_1\omega_2}{\omega_1+\omega_2}$ and $a_1 = \frac{2\zeta}{\omega_1+\omega_2}$

5. Train properties are read (HSLM A1:A10, mass of the vehicle part, mass of suspensions and wheel, suspension stiffness and suspension damping). The model HSLM-A1 is used in the forthcoming numerical study with the properties: number of intermediate coaches (N) = 18, coach length (D) = 18 m, bogie axle spacing (d) = 2 m and the axle point load (P) = 170 kN. Mass of the vehicle part is taken as a ratio of the mass of the axle by comparison to the same ratio in real high-speed trains (nearly 75 ~ 78%).
6. All initial values of the bridge structure and vehicles are set to zero.
7. For each time step Δt, each axle moves a distance Δx. The new position of each axle is determined and shape functions $\langle N_c \rangle$ (Hermitian cubic interpolation) for the positions of contact points with each element are calculated as:

$$\langle Nc \rangle = \langle N_1\ N_2\ N_3\ N_4 \rangle$$

$N_1 = 1 - 3(x/l)^2 + 2(x/l)^3$, $N_2 = x - 2x^2/l + x^3/l^2$, $N_3 = 3(x/l)^2 - 2(x/l)^3$, $N_4 = -x^2/l + x^3/l^2$,

where x is the distance of the axle from the element start node and l is the size of the element.

8. The deformations under the contact points on the bridge elements ($u_{contact}$) are calculated from the bridge deformation in the previous time step (t-Δt) using the shape functions.

$$u_{contact} = N_c\{u\}_{element}$$

9. The deformations of the contact points (u_1) are then calculated by adding the rail irregularities (r) to the deformations under the contact points on the bridge elements ($u_{contact}$).

$$u_1 = u_{contact} + r$$

10. The partitioned matrices of the vehicle system's upper parts are then solved by time integration using Newmark's β method.

$$M_{uu}\ddot{U}_{u_{t+\Delta t}} + C_{uu}\dot{U}_{u_{t+\Delta t}} + K_{uu}U_{u_{t+\Delta t}} = F_{u_{t+\Delta t}} - K_{ul}U_{l_{t+\Delta t}} = F_{t+\Delta t}$$

$U_{l_{t+\Delta t}}$ was determined in step (9) which equals $\{u_1\}$ and $F_{u_{t+\Delta t}} = \begin{bmatrix}0\\0\end{bmatrix}$

$$[F]_{t+\Delta t} = F_{u_{t+\Delta t}} - K_{ul}U_{l_{t+\Delta t}} = -K_{ul}U_{l_{t+\Delta t}} = \begin{bmatrix}k_{ballast}\\0\end{bmatrix}\{u_1\} = \begin{bmatrix}k_{ballast}\times u_1\\0\end{bmatrix}$$

$$[K_{eff}] = \frac{4}{\Delta t^2}M_{uu} + \frac{2}{\Delta t}C_{uu} + K_{uu}$$

$$[F_{eff}]_{t+\Delta t} = [F]_{t+\Delta t} + M_{uu}\left\{\frac{4}{\Delta t^2}U_{u_t} + \frac{4}{\Delta t}\dot{U}_{u_t} + \ddot{U}_{u_t}\right\} + C_{uu}\left\{\frac{2}{\Delta t}U_{u_t} + \dot{U}_{u_t}\right\}$$

$$U_{u_{t+\Delta t}} = [K_{eff}]^{-1} \times [F_{eff}]_{t+\Delta t}$$

$$\ddot{U}_{u_{t+\Delta t}} = \frac{4}{\Delta t^2}\{U_{u_{t+\Delta t}} - U_{u_t}\} - \frac{4}{\Delta t}\dot{U}_{u_t} - \ddot{U}_{u_t}\dot{U}_{u_{t+\Delta t}} = \dot{U}_{u_t} + \frac{\Delta t}{2}\ddot{U}_{u_t} + \frac{\Delta t}{2}\ddot{U}_{u_{t+\Delta t}}$$

11. Once the response of the vehicle system is calculated, the dynamic contact force (f_{dyn}) can be calculated from the lower part matrix as:

$$K_{ll}U_{l_{t+\Delta t}} = F_{l_{t+\Delta t}} - K_{lu}U_{u_{t+\Delta t}}$$

Rearranging yields:

$$F_{l_{t+\Delta t}} = K_{lu}U_{u_{t+\Delta t}} + K_{ll}U_{l_{t+\Delta t}} = f_{dyn}$$

12. The contact forces exerted by each vehicle axle on the bridge elements are then calculated.

$$f_{contact} = f_{dyn} + f_{stat}$$

13. The nodal forces are found for each element according to the value of contact force and shape function of the contact point:

$$f_{bridge} = \{N_c\} \times f_{contact}$$

14. Force matrix for the bridge system is constructed and the bridge system is then solved using Newmark's

β method as in step (10) to find the response of the bridge.

15. Convergence for dynamic force is checked. If convergence is satisfied, we move forward to the new time step; otherwise, we loop about step (8) to get the new f_{dyn} and response for the new iteration.

$$\frac{f_{dyn}^{i+1} - f_{dyn}^{i}}{f_{dyn}^{i}} < required\ tolerance$$

It is worth noting that using a proper element size can lead to the required accuracy without need to make time-consuming iterations.

The two methods of solution along with the simple dynamic analysis of moving load case are developed as MATLAB® codes.

NUMERICAL STUDY

The dynamic analysis of a high-speed railway continuous non-prismatic bridge of prestressed concrete using the HSLM-A1 will be adopted to make an assessment for the bridge and the passing train. Two interaction models plus a moving-load model will be compared.

Bridge and Train Parameters

The bridge has an overall length of 118 m with two spans of 59 m each and a box section of variable height and thickness, as shown in Fig. 5. Modulus of elasticity of prestressed concrete will be 30.1 GPa and 1% damping ratio will be used. Each axle of the HSLM-A1 will have the following properties: M_v = 13000 kg, M_w = 4329.25 kg, K_v = 1200 kN/m and C_V = 85 kN.s/m. The bridge will be exposed to the passage of the HSLM A1 train and studied for speeds ranging from 20 to 140 m/s (72 to 504 km/h).

RESULTS

Interaction and Non-interaction Modeling

Figs. 6.a and 6.b of maximum deflection and acceleration of the bridge show that the three models give very similar responses except at resonance speeds. At resonance speeds, the moving-load model shows a much higher response of the bridge than the other two models (interaction models) and tends to be more conservative. The lower response of interaction models may be due to the decrease in external excitation caused by the absorption of energy in the track elastic properties and in the spring-damper unit of the suspension.

Also, the moving-load model shows resonance at slightly higher speeds than the interaction models for two reasons: the first is that the added mass from train to bridge causes the whole system to have a lower natural frequency than the bridge alone; hence, interaction models show resonance with train load pattern at lower speeds, while the second reason is that the track elastic properties along with the suspension of the vehicle system cause a reduction in the whole system stiffness, which means a decrease in the natural frequency of the whole system. It is shown that the first resonance in moving-load model occurs at a speed of 32 m/s (115.2 km/h), but in interaction models, the first resonance occurs at a speed of 30.5 m/s (109.8 km/h). Meanwhile, another resonance occurs at a speed of 129.5 m/s (466.2 km/h) for the moving-load model and at a speed of 128 m/s (460.8 km/h) for both interaction models.

Concerning the bridge response, an important serviceability criterion is the deck acceleration. As recommended in the Annex A2 of EN 1990, deck acceleration shouldn't exceed 3.5 m/s^2 for ballasted tracks and 5.0 m/s^2 for directly fastened decks with the track and structural elements designed for high-speed traffic.

As for the vehicle response, riding comfort is measured by the car body acceleration. Annex A2 of EN-1990 suggests 3 levels for comfort: *i*) Very good, *ii*) Good, *iii*) Acceptable, corresponding to the vertical accelerations: 1, 1.3 and 2 m/s^2, respectively. The Bureau of Taiwan High-speed Railways set a limit of 0.05 g (0.49 m/s^2) for the comfort of passengers (Yang et al., 2004).

In general, the vertical acceleration of the vehicle increases with the speed of the train, as Fig. 6.c indicates. So, this comfort criterion is crucial in limiting the running speed of the train.

Track Vertical Irregularities

Three profiles of vertical irregularities are compared for results: a) PSD function class 6, b) PSD function class 5, c) periodic function, as shown in Fig. 7. The quality of track depends on the value of irregularities and their pattern. Track of class 5 has higher values than that of class 6. Periodic irregularities are a hypothetical case of track unevenness which may be considered in the analysis. Amplitude of irregularity function and its wavelength define the quality of track in comparison with the six classes of random PSD function of irregularity.

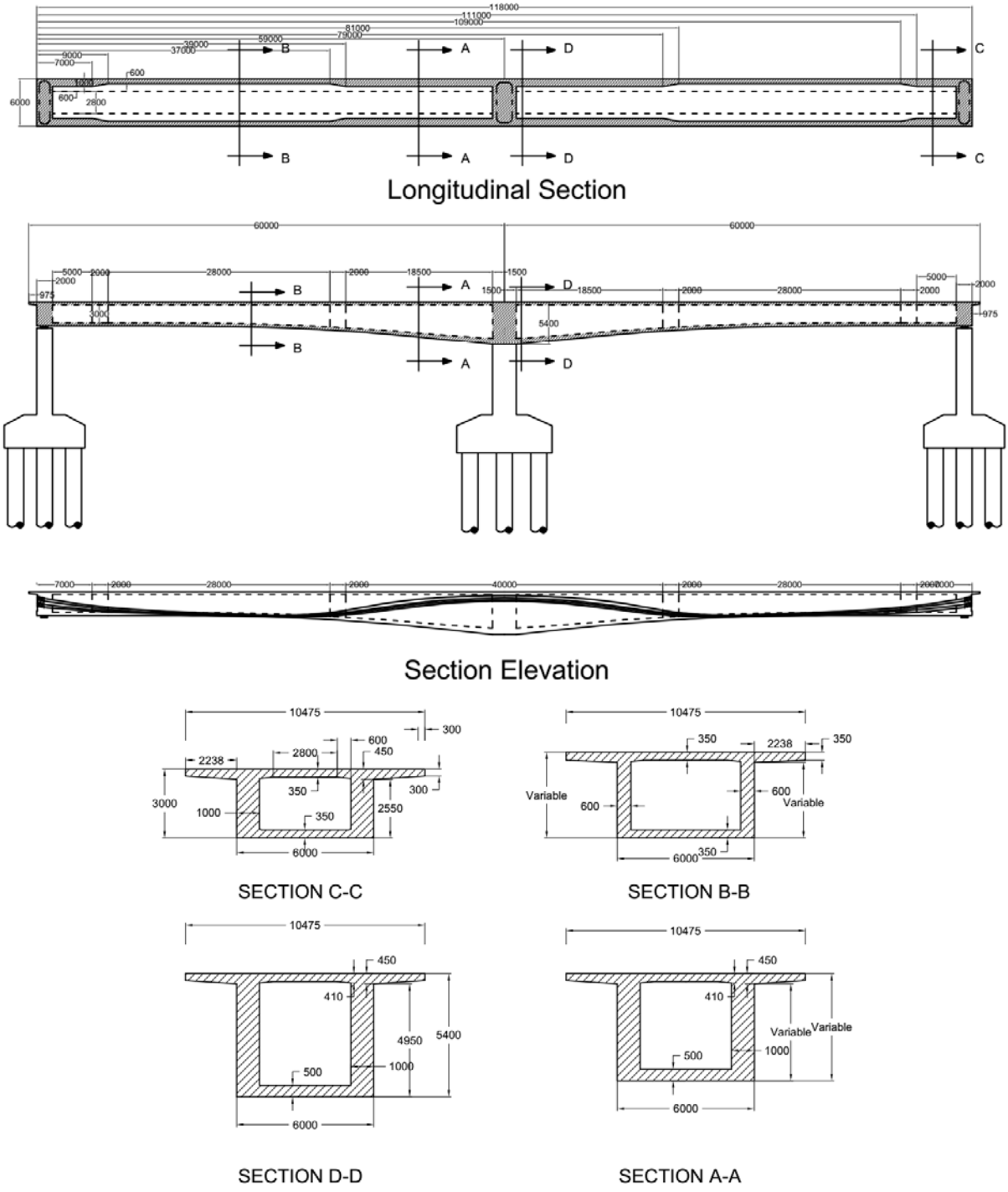

Figure (5): Bridge geometry and cross-sections

Track irregularities have a small or insignificant effect on the bridge response, especially the bridge deflection, as Figs. 8.a and 8.b indicate. The effect of irregularities on bridge deck acceleration is greater than that on bridge deflection, but both are still insignificant. The impact between vehicle and bridge increases with more irregularities; thus, the track with class 5 shows a higher response than the track with class 6. On the other side, vehicle response is highly affected by irregularities.

These irregularities caused a higher vertical acceleration of the train, which in turn limits the running

speed to meet the requirements of riding comfort, as shown in Fig. 8.c. Applying the comfort criterion of max. acceleration of 0.05g (0.49 m/s^2), the running speed will be limited to:

- 82.64 m/s (297.5 km/h) for no irregularities of the track.
- 73.81 m/s (265.7 km/h) for class-6 track.
- 69.64 m/s (250.7 km/h) for periodic irregularities of the track.
- 59.42 m/s (213.9 km/h) for class-5 track.

It is shown that high classes of tracks – regarding irregularities – are preferable for high-speed lines.

Track Stiffness

Four values of track stiffness (20, 40, 80 and 160) kN/mm are applied with no track irregularities included. Results of analysis show that track stiffness has a minimal effect on the bridge response; however, it mitigates the impact between train and bridge, so it tends to give a relatively lower response for low-track stiffness as in Figs. 9.a and 9.b. In contrast, the train response is higher for low-track stiffness due to the softening effect added by the low-ballast stiffness. The higher response of the train appears directly in train deflection and not in acceleration, as the results in Figs. 9.c and 9.d reveal.

(a)

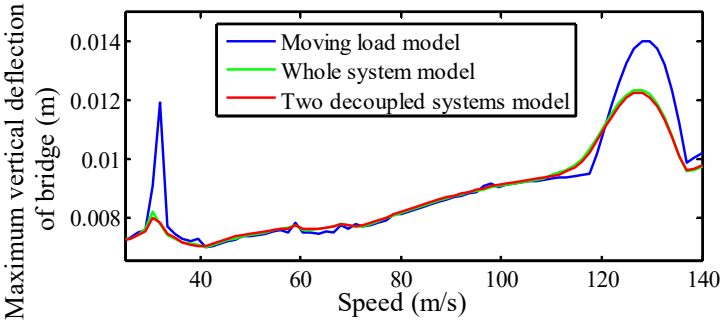

(b)

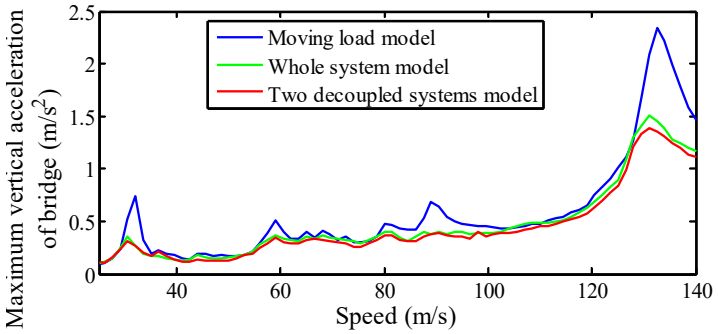

(c)

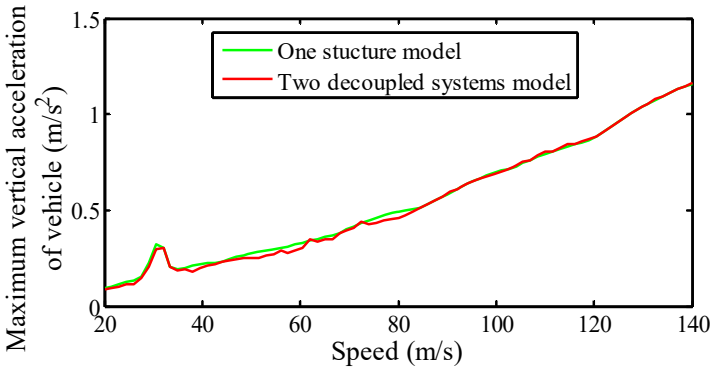

Figure (6): (a) Bridge maximum deflection, (b) Bridge maximum acceleration and (c) Maximum vertical vehicle acceleration

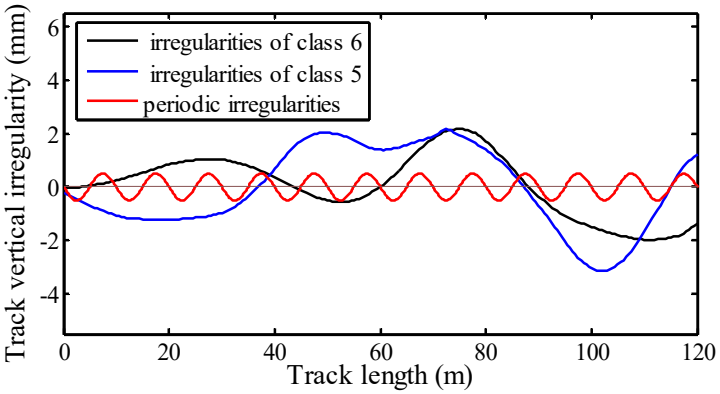

Figure (7): Different profiles for track irregularities

(a)

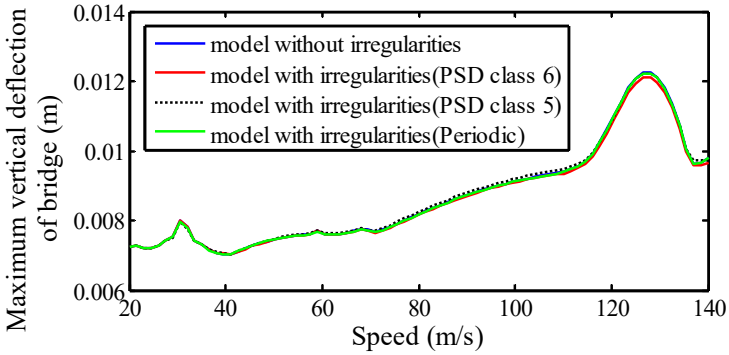

(b)

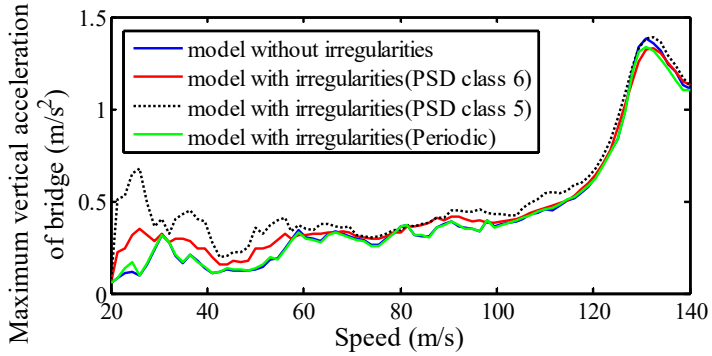

(c)

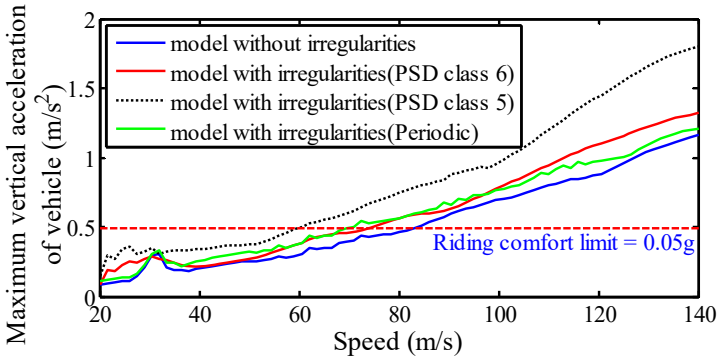

Figure (8): (a) Bridge maximum deflection, (b) Bridge maximum acceleration and (c) Maximum vertical vehicle acceleration for different profiles of track irregularities

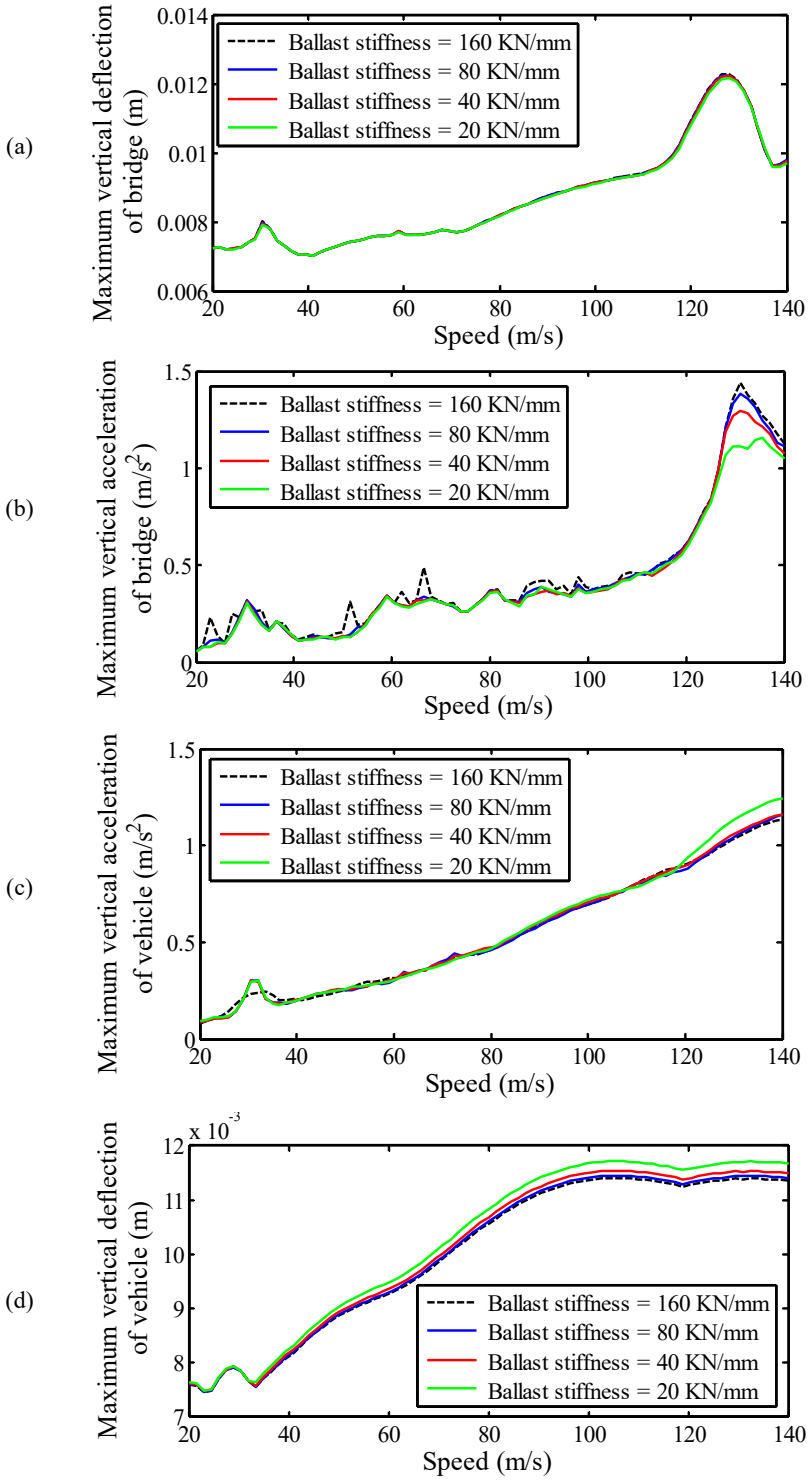

Figure (9): (a) Bridge maximum deflection, (b) Bridge maximum acceleration, (c) Vehicle maximum acceleration and (d) Vehicle maximum deflection for different track stiffness values

Vehicle Suspension

Four values of suspension stiffness (800, 1200, 1800 and 2500) kN/m were applied with no track irregularities included and with ballast stiffness of 80 kN/mm. Response Figures; Figs. 10.a, 10.b, 10.c and 10.d indicate that train system is mainly influenced by the suspension stiffness. Higher suspension stiffness gives higher vehicle acceleration at all speeds and higher deflection only at high resonance speeds, but relatively lower deflection at speeds with no resonance as

expected. Bridge response is barely affected, but stiffer suspension can slightly mitigate the bridge response, especially at resonance speeds.

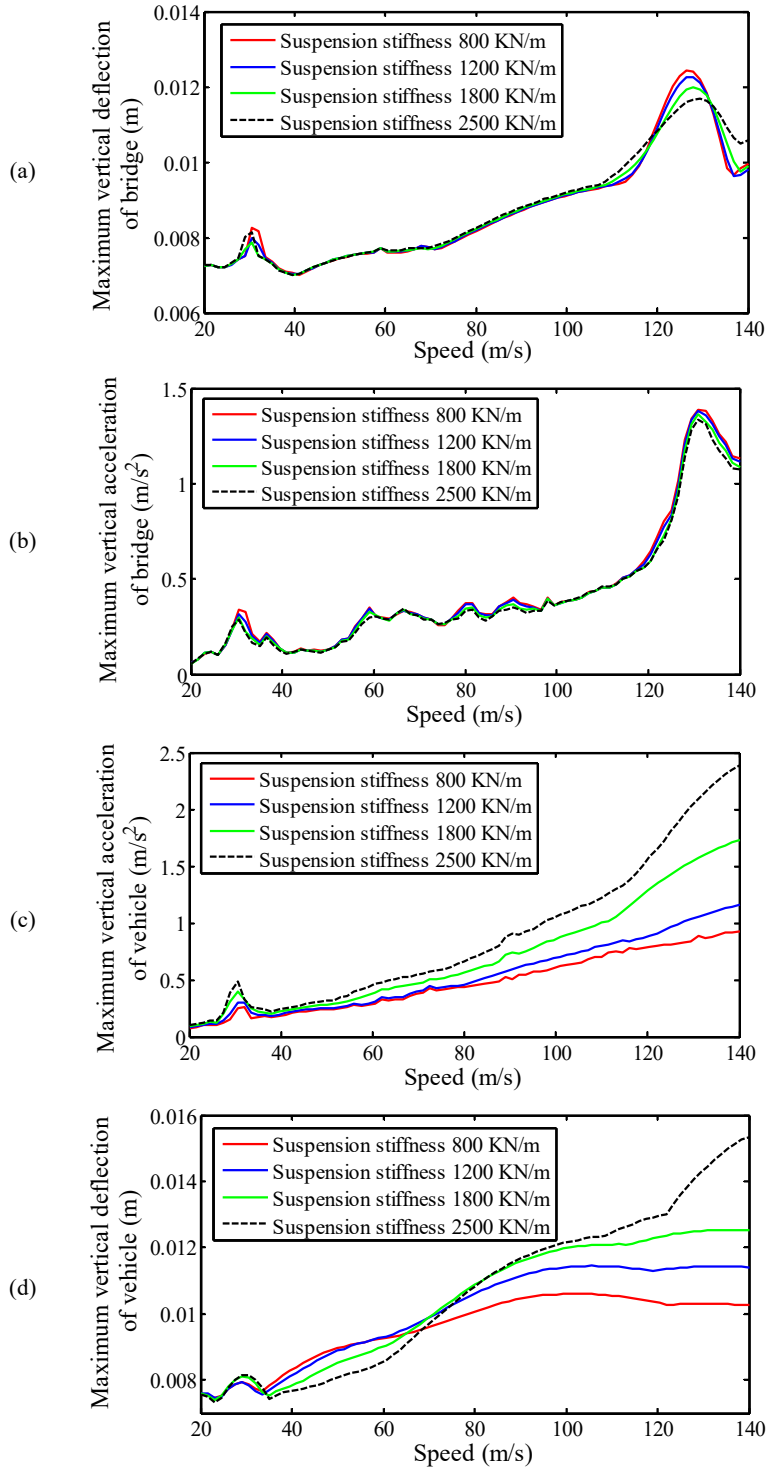

Figure (10): (a) Bridge maximum deflection, (b) Bridge maximum acceleration, (c) Vehicle maximum acceleration and (d) Vehicle maximum deflection for different suspension stiffness values

Envelope Response of HSLM-A Family vs. Real High-speed Trains

Fixing the following parameters: K_v = 1200 kN/m, C_V = 85 kN.s/m, $K_{ballast}$ = 80 kN/mm and class 6 for track irregularities, the whole train family HSLM-A is applied for the dynamic analysis to obtain the bridge response envelope as given in Fig. 11.a and Fig. 11.b.

(a)

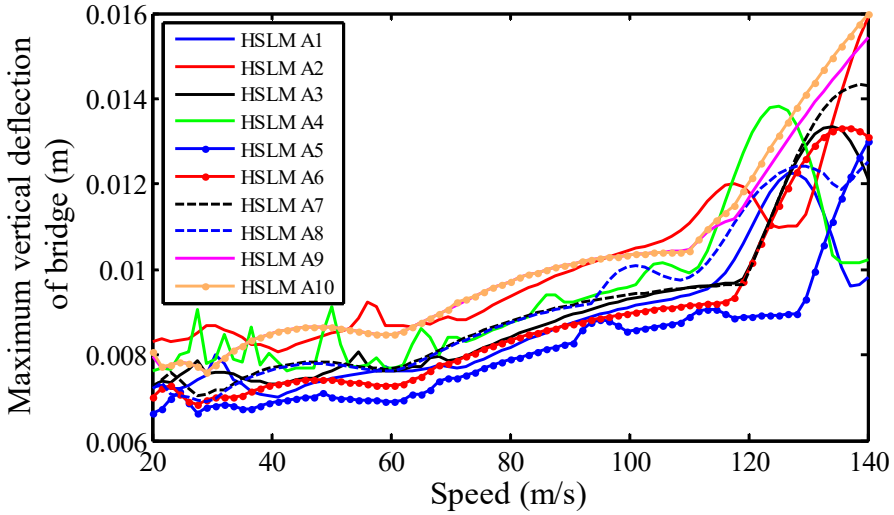

(b)

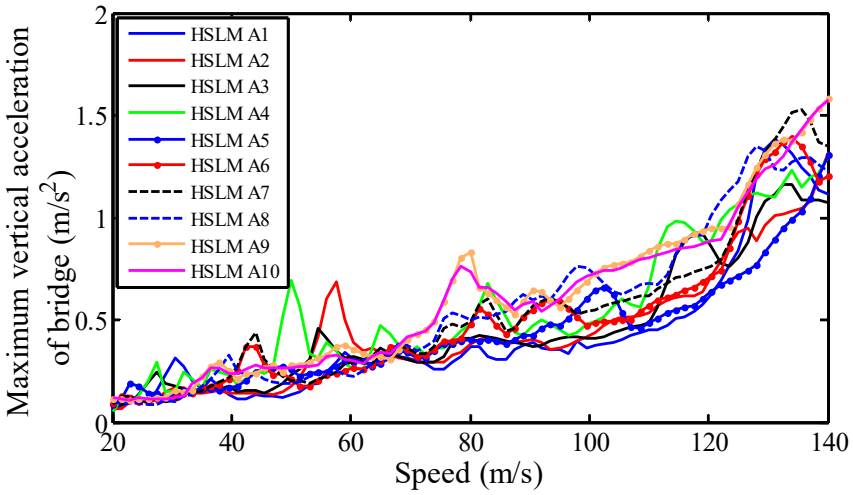

Figure (11): (a) Maximum bridge deflection for different HSLM trains and (b) Maximum bridge deck acceleration for different HSLM trains

Four real trains are adopted for the dynamic analysis to test the ability of the HSLM-A family to envelop the signature of present and prospective high-speed trains. The four high-speed trains are the Chinese train CRH380A for which the maximum speed is 380 km/h, the Japanese series N700-I train for which the maximum speed is 330 km/h, the German Inter-City Express 3 (ICE-3) for which the maximum service speed is 320 km/h and Bombardier Zefiro 380 for which the maximum service speed is 380 km/h. Each train comprises eight cars with a total of 16 bogies and 32 wheelsets.

The envelope response of the HSLM-A family is relatively surpassed by the response under the action of the Bombardier Zefiro 380, but at a relatively low speed. At high speeds, the envelope response can be reliable with very small surpassings regarding the acceleration response as shown in Fig. 12.a and Fig. 12.b.

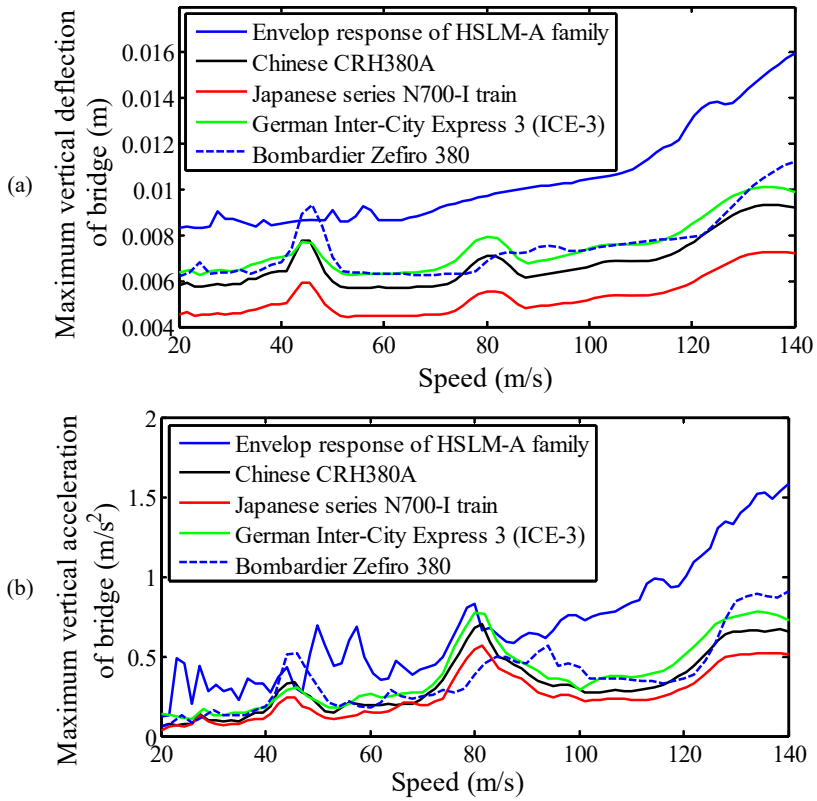

Figure (12): (a) Envelope of deflection response of HSLM-A family compared with the response of individual real high-speed trains and (b) Envelope of acceleration response of HSLM-A family compared with the response of individual real high-speed trains

CONCLUSIONS

Investigation of the dynamic response of railway bridges exposed to high-speed trains is attracting more attention recently. Various models and solution techniques for the dynamic problem were developed. Complex models are the most precise ones, but they are time-consuming and not suitable for preliminary stages of design or assessment. In this paper, two methods for solving the nonlinear coupled interaction problem of train passage over a bridge were studied. The two methods are different in the way they work. The first is a non-iterative method which deals with the entire system and updates the system matrices at each time step. The other method is iterative and decouples the two interacting systems through contact forces and permanent contact criteria. Along with the moving load model, the two interaction methods are applied for dynamic analysis. Results show that the two interaction models give very similar responses for bridge and train. The moving-load model tends to overestimate the response of the bridge at resonance speeds and shows resonance at slightly higher speeds than the interaction models. Irregularities of the track are of great impact on the riding comfort and can cause very high vibrations in the train coaches at high-speeds; hence, higher classes of tracks with less irregularities are preferred for high-speed railway lines. The elastic property of the ballasted track adds a softening effect to the whole system and provides a slight mitigation of the response of both systems. The stiffness of the train suspension has a great effect on the train response only, but a minimal effect on the bridge response. The response envelope under the excitation of the 10 HSLM-A trains can generally be trustworthy, but can be slightly surpassed by some real train response when interaction models are adopted at some low speeds.

REFERENCES

Atashafrazeh, M., and Shirmohammadi, H. (2016). "2D modeling and analysis of railway track under subjected loads". Jordan Journal of Civil Engineering, 10 (3), 290-296.

Delgado, R.M., & Dos Santos, R.C.S.M. (1997). "Modeling of railway bridge-vehicle interaction on high-speed tracks". Computers and Structures, 63 (3), 511-523.

EN 1991-2. (2003). "Eurocode 1: Actions on structures - Part 2: Traffic loads on bridges".

European Rail Research Institute (ERRI). (1999). "Rail bridges for speeds over 200 km/h". Final Report, ERRI D214/RP 9.

Frýba, L. (1999). "Vibration of solids and structures under moving load". 3rd Edition, London, Thomas Telford.

Gu, G. (2015). "Resonance in long-span railway bridges carrying TGV trains". Computers and Structures, 152, 185-199. https://doi.org/10.1016/j.compstruc.2015.02.002

Lei, X., and Noda, N.A. (2002). "Analyses of dynamic response of vehicle and track coupling system with random irregularity of track vertical profile". Journal of Sound and Vibration, 258 (1), 147-165.

Lou, P., and Zeng, Q. Y. (2005). "Formulation of equations of motion of finite element form for vehicle-track-bridge interaction system with two types of vehicle model". International Journal for Numerical Methods in Engineering, 62 (3), 435-474.

Neves, S.G.M., Montenegro, P.A., Azevedo, A.F.M., and Calçada, R. (2014). "A direct method for analyzing the nonlinear vehicle-structure interaction". Engineering Structures, 69, 83-89.

Newmark, N.M. (1959). "Method of computation for structural dynamics". Proceedings of the American Society of Civil Engineers, 67-94.

Nour, S.I., and Issa, M.A. (2016). "High-speed rail short bridge-track-train interaction based on the decoupled equations of motion in the finite-element domain". ASME 2016 Joint Rail Conference, JRC2016-5785, Columbia, SC, USA, April 12-15, 1-15.

Olmos, J.M., and Astiz, M. (2018). "Non-linear vehicle-bridge-wind interaction model for running safety assessment of high-speed trains over a high-pier viaduct". Journal of Sound and Vibration, 419, 63-89. https://doi.org/10.1016/j.jsv.2017.12.038

Podwórna, M. (2015). "Modeling of random vertical irregularities of railway tracks". International Journal of Applied Mechanics and Engineering, 20 (3), 647-655. https://doi.org/10.1515/ijame-2015-0043

Timoshenko, S.P., and Young, D.H. (1955). "Vibration problems in engineering". 3rd Edn., New York, D. Van Nostrand.

Wu, Y.S., Yang, Y.B., and Yau, J.D. (2001). "Three-dimensional analysis of train-rail-bridge interaction problems". Vehicle System Dynamics, 36 (1), 1-35.

Wu, Yean Seng, and Yang, Y. Bin. (2003). "Steady-state response and riding comfort of trains moving over a series of simply supported bridges". Engineering Structures, 25, 251-265.

Xia, H., Zhang, N., and De Roeck, G. (2003). "Dynamic analysis of high-speed railway bridge under articulated trains". Computers and Structures, 81 (26-27), 2467-2478.

Yang, Y. Bin, Chang, C.H., and Yau, J.D. (1999). "An element for analyzing vehicle-bridge systems considering vehicle's pitching effect". International Journal for Numerical Methods in Engineering, 46, 1031-1047.

Yang, F., and Fonder, G.A. (1996). "An iterative solution method for dynamic response of bridge-vehicle systems". Earthquake Engineering and Structural Dynamics, 25, 195-215.

Yang, Y.B., and Lin, B.-H. (1995). "Vehicle-bridge interaction analysis by dynamic condensation method". Journal of Structural engineering, 121 (11), 1636-1643.

Yang, Y.B., Yau, J.D., and Wu, Y.S. (2004). "Vehicle-bridge interaction dynamics with applications to high-speed railways". Singapore, World Scientific Publishing Co.

Zeng, Z.P., Liu, F.S., Lou, P., Zhao, Y.G., and Peng, L.M. (2016). "Formulation of three-dimensional equations of motion for train-slab track-bridge interaction system and their application to random vibration analysis". Applied Mathematical Modeling, 40, 5891-5929.

Zhai, W., Han, Z., Chen, Z., Ling, L., and Zhu, S. (2019). "Train–track–bridge dynamic interaction: A state-of-the-art review". Vehicle System Dynamics, 57(7), 984–1027.

Zhang, Q.L., Vrouwenvelder, A., and Wardenier, J. (2001). "Numerical simulation of train-bridge interactive dynamics". Computers and Structures, 79 (10), 1059-1075.